International Journal on "Technical and Physical Problems of Engineering" (IJTPE)
Published by International Organization on TPE (IOTPE)

ISSN 2077-3528
IJTPE Journal
www.iotpe.com
ijtpe@iotpe.com

September 2010 | Issue 4 | Volume 2 | Number 3 | Pages 82-87

DAMPING FUNCTION OF BACK TO BACK HVDC BASED VOLTAGE SOURCE CONVERTER

N.M. Tabatabaei [1] N. Taheri [2] N.S. Boushehri [1]

1 Electrical Engineering Department, Seraj Higher Education Institute, Tabriz, Iran
n.m.tabatabaei@gmail.com, n.s.boushehri@gmail.com
2 Islamic Azad University, Ghouchan Branch, Ghouchan, Iran, n.taheri.1362@gmail.com

Abstract- This paper presents the establishment of linearised Phillips-Heffron model of a power system installed HVAC parallel-connected with a Back To Back High Voltage Direct Current based voltage source converter (BtB VSC HVDC). The use of the supplementary controllers of a BtB VSC HVDC to damp low frequency oscillations in a weakly connected system is considered. The potential of the BtB VSC HVDC supplementary controllers to enhance the dynamic stability is evaluated using damping function.

Keywords: Phillips-Heffron Model, Back To Back, HVAC, BtB VSC HVDC.

I. INTRODUCTION

As power demand grows rapidly and expansion in transmission and generation is restricted with the limited availability of resources and the strict environmental constraints, power systems are today much more loaded than before. This causes the power systems to be operated near their stability limits [1]. Power system stabilizers (PSSs) aid in maintaining power system stability and improving dynamic performance by providing a supplementary signal to the excitation system [2].

However, PSSs may adversely affect voltage profile, may result in leading power factor, and may not be able to suppress oscillations resulting from severe disturbances, especially those three-phase faults which may occur at the generator terminals [1].

The availability of Flexible AC Transmission System (FACTS) controllers, such as Static VAR Compensators (SVC), Thyristor Control Series Compensators (TCSC), Static Synchronous Compensators (STATCOM), and Unified Power Flow Controller (UPFC), have led their use to damping oscillations [3-5].

Extremely fast control action associated with FACTS-device operations, they have been very promising candidates for utilization in power system damping enhancement. It has been observed that utilizing a feedback supplementary control, in addition to the FACTS-device primary control, can considerably improve system damping and can also improve system voltage profile, which is advantageous over PSSs [1].

Recently HVDC systems have greatly increased. They interconnect large power systems offering numerous technical and economic benefits. This interest results from functional characteristics and performance that include for example nonsynchronous interconnection, control of power flow and modulation to increase stability limits [6]. It is well known that the transient stability of the AC systems in a composite AC-DC system can be improved by taking advantage of the fast controllability of HVDC converters [7-12]. There are, therefore, good reasons for constructing HVDC links in close proximity to HVAC lines.

In this paper a novel approach is presented to model parallel-connected HVAC and BtB VSC HVDC systems. In addition to the state-space representation, a block diagram representation is formed to analyze the system stability characteristics. By this modeling approach, it is possible to analyze the small-signal stability of the system and low-frequency oscillation phenomena with the synchronous machine.

II. CONFIGURATION OF POWER SYSTEM

Figure 1 shows a SMIB system equipped with a HVDC. The four input control signals to the HVDC are M_r, PH_r, M_i, PH_i where M_r, M_i are the amplitude modulation ratio and PH_r, PH_i are phase angle of the control signals of each VSC respectively.

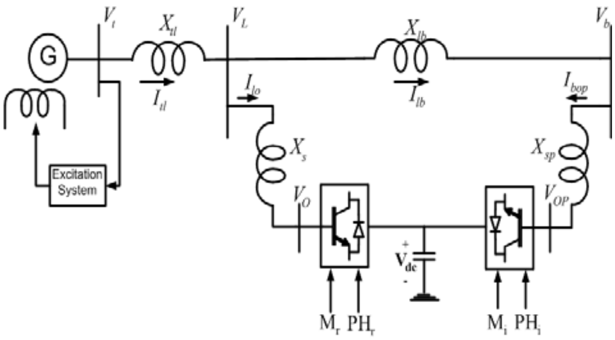

Figure 1. Configuration of case study

By applying Park's transformation and neglecting the resistance and transients of the coupling transformers, the HVDC can be modeled:

$$\begin{bmatrix} V_{Ld} \\ V_{Lq} \end{bmatrix} = \begin{bmatrix} 0 & -X_s \\ X_s & 0 \end{bmatrix} \begin{bmatrix} I_{lod} \\ I_{loq} \end{bmatrix} + \begin{bmatrix} \frac{M_r V_{dc} \cos(PH_r)}{2} \\ \frac{M_r V_{dc} \sin(PH_r)}{2} \end{bmatrix} \quad (1)$$

$$\begin{bmatrix} V_{bd} \\ V_{bq} \end{bmatrix} = \begin{bmatrix} 0 & -X_{sp} \\ X_{sp} & 0 \end{bmatrix} \begin{bmatrix} I_{bopd} \\ I_{bopq} \end{bmatrix} + \begin{bmatrix} \frac{M_i V_{dc} \cos(PH_i)}{2} \\ \frac{M_i V_{dc} \sin(PH_i)}{2} \end{bmatrix} \quad (2)$$

$$C_{dc} \dot{V}_{dc} = [\frac{M_r}{2}(I_{lod} \cos(PH_r) + I_{loq} \sin(PH_r)) + \frac{M_i}{2}(I_{bopd} \cos(PH_i) + I_{bopq} \sin(PH_i))] \quad (3)$$

where V_L, V_b, I_{lo} and I_{bo} are the middle bus voltage, infinite bus voltage, flowed current to rectifier and inverter respectively. C_{dc} And V_{dc} are the DC link capacitance and voltage, respectively.

The non-linear model of the SMIB system of Figure1 is:

$$\dot{\delta} = \omega_b \omega \quad (4)$$

$$\dot{\omega} = \frac{(P_m - P_e - D\omega)}{M} \quad (5)$$

$$\dot{E}_q' = \frac{(E_{fd} - (x_d - x_d')I_{td} - E_q')}{T_{do}'} \quad (6)$$

$$\dot{E}_{fd} = \frac{(K_A(V_{ref} - V_t) - E_{fd})}{T_A} \quad (7)$$

where $P_e = V_{td} I_{td} + V_{tq} I_{tq}$, $V_t = \sqrt{V_{td}^2 + V_{tq}^2}$, $V_{td} = x_q I_{tq}$, $V_{tq} = E_q' - x_d' I_{td}$, $I_{td} = I_{lod} + I_{bd}$, $I_{tq} = I_{loq} + I_{bq}$ and P_m and P_e are the input and output power, respectively; M and D the inertia constant and damping coefficient, respectively; ω_b the synchronous speed; δ and ω the rotor angle and speed, respectively; E_q', E_{fd} and V_t the generator internal, field and terminal voltages, respectively; T_{do}' the open circuit field time constant; X_d, X_d' and X_q the d-axis, d-axis transient reactance, and q-axis reactance, respectively; K_A and T_A the exciter gain and time constant, respectively; V_{ref} the reference voltage. Also, from Figure1 we have:

$$\bar{V}_t = jX_{tl} \bar{I}_{tl} + \bar{V}_l \quad (8)$$

$$\bar{V}_t = jX_{tl} \bar{I}_{tl} + jX_{lb} \bar{I}_{lb} + \bar{V}_b \quad (9)$$

$$\bar{I}_{lb} = \bar{I}_{tl} - \frac{\bar{V}_t - jX_{tl} \bar{I}_{tl} - \bar{V}_o}{jX_s} \quad (10)$$

Where $\bar{I}_{tl}$, $\bar{V}_o$, $\bar{I}_{lb}$ and $\bar{V}_b$ are the armature current, rectifier voltage, infinite bus current and voltage respectively. From (8)-(10) we can have:

$$I_{tlq} = \frac{\frac{X_{lb}}{X_s} \frac{M_r}{2} V_{dc} \cos(PH_r) + V_b \sin(\delta)}{ZX_q + A} \quad (11)$$

$$I_{tld} = \frac{ZE_q' - \frac{X_{lb}}{X_s} \frac{M_r}{2} V_{dc} \sin(PH_r)}{ZX_d' + A} - \frac{-V_b \cos(\delta)}{ZX_d' + A} \quad (12)$$

And for inverter side:

$$I_{bopd} = \frac{V_b \cos(\delta) - \frac{M_i}{2} V_{dc} \sin(PH_i)}{X_{sp}} \quad (13)$$

$$I_{bopq} = -\frac{V_b \sin(\delta) - \frac{M_i}{2} V_{dc} \cos(PH_i)}{X_{sp}} \quad (14)$$

By linearising (1)-(7), (11)-(14):

$$\Delta\dot{\delta} = \omega_b \Delta\omega \quad (15)$$

$$\Delta\dot{\omega} = \frac{(\Delta P_m - \Delta P_e - D\Delta\omega)}{M} \quad (16)$$

$$\Delta\dot{E}_q' = \frac{(\Delta E_{fd} - (x_d - x_d')\Delta I_{td} - \Delta E_q')}{T_{do}'} \quad (17)$$

$$\Delta\dot{E}_{fd} = \frac{(K_A \Delta V_t - \Delta E_{fd})}{T_A} \quad (18)$$

where

$$\Delta\dot{V}_t = K_5 \Delta\delta + K_6 \Delta E_q' + K_{Vdc} \Delta V_{dc} + K_{VM_r} \Delta M_r + K_{VPHr} \Delta PH_r \quad (19)$$

$$\Delta P_e = K_1 \Delta\delta + K_2 \Delta E_q' + K_{pdc} \Delta V_{dc} + K_{pMr} \Delta M_r + K_{pPHr} \Delta PH_r \quad (20)$$

$$\Delta E_q = K_3 \Delta E_q' + K_4 \Delta\delta + K_{qPHr} \Delta PH_r + K_{qMr} \Delta M_r + K_{qdc} \Delta V_{dc} \quad (21)$$

$$\Delta\dot{V}_{dc} = q_1 \Delta\delta + q_2 \Delta E_q' + q_3 \Delta V_{dc} + q_4 \Delta M_r + q_5 \Delta PH_r + q_6 \Delta M_i + q_7 \Delta PH_i \quad (22)$$

Substitute (19)-(22) in (15)-(18) we can obtain the state variable of the power system installed with the BtB VSC HVDC to be in Equation (23) where $\Delta M_i, \Delta M_r, \Delta PH_i$ and ΔPH_r are the linearization of the input control signals of the BtB VSC HVDC. The linearised dynamic model of (23) can be shown by Figure 2.

$$\begin{bmatrix} \dot{\Delta\delta} \\ \dot{\Delta\omega} \\ \dot{\Delta E_q'} \\ \dot{\Delta E_{fd}} \\ \dot{\Delta V_{dc}} \end{bmatrix} = \begin{bmatrix} 0 & \omega_b & 0 & 0 & 0 \\ -\frac{K_1}{M} & -\frac{D}{M} & -\frac{K_2}{M} & 0 & -\frac{K_{pdc}}{M} \\ -\frac{K_4}{T_{do}'} & 0 & -\frac{K_3}{T_{do}'} & \frac{1}{T_{do}'} & -\frac{K_{qdc}}{M} \\ -\frac{K_A T_A}{T_A} & 0 & -\frac{K_A K_6}{T_A} & -\frac{1}{T_A} & -\frac{K_A K_{Vdc}}{T_A} \\ q_1 & 0 & q_2 & 0 & q_3 \end{bmatrix} . \begin{bmatrix} \Delta\delta \\ \Delta\omega \\ \Delta E_q' \\ \Delta E_{fd} \\ \Delta V_{dc} \end{bmatrix}$$

$$+ \begin{bmatrix} 0 & 0 & 0 & 0 \\ -\frac{K_{pMr}}{M} & -\frac{K_{pPHr}}{M} & 0 & 0 \\ -\frac{K_{qMr}}{T_{do}'} & -\frac{K_{qPHr}}{T_{do}'} & 0 & 0 \\ -\frac{K_A K_{VMr}}{T_A} & -\frac{K_A K_{VPHr}}{T_A} & 0 & 0 \\ q_4 & q_5 & q_6 & q_7 \end{bmatrix} . \begin{bmatrix} \Delta M_r \\ \Delta PH_r \\ \Delta M_i \\ \Delta PH_i \end{bmatrix} \tag{23}$$

In this figure $K_{pu}, K_{qu}, K_{vu}, K_q$ and ΔU are defined below:

$K_{pu} = [K_{pMr}, K_{pPHr}, 0, 0]'$

$K_{qu} = [K_{qMr}, K_{qPHr}, 0, 0]'$

$K_{vu} = [K_{VMr}, K_{VPHr}, 0, 0]'$

$K_q = [q_4, q_5, q_6, q_7]'$

$\Delta U = [\Delta M_r, \Delta PH_r, \Delta M_i, \Delta PH_i]$

It can be seen that the configuration of the Phillips-Heffron model is exactly the same as that installed with SVC, TCSC, TCPS, UPFC and STATCOM.

Also from (23) it can be seen that there are four choice of input control signals of the BtB VSC HVDC to superimpose on the damping function of the BtB VSC HVDC $\Delta M_i, \Delta M_r, \Delta PH_i$ and ΔPH_r. Therefore, in designing the damping controller of the BtB VSC HVDC, besides setting its parameters, the selection of the input control signal of the BtB VSC HVDC to superimpose on the damping function of the BtB VSC HVDC is also important.

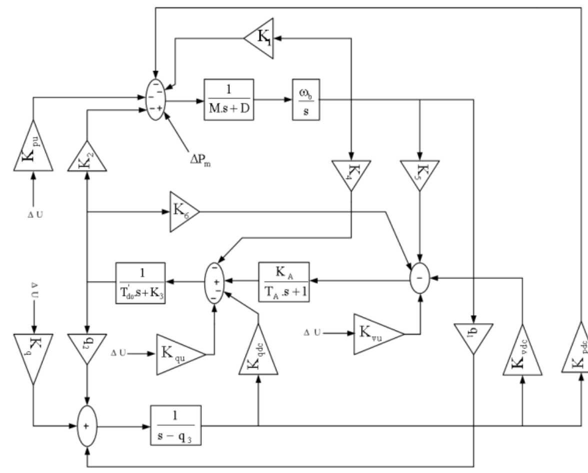

Figure 2. Phillips-Heffron model of power system installed with HVDC

III. BTB VSC HVDC DAMPING FUNCTION

The linearised model of the power system installed with the BtB VDC HVDC can be expressed by Figure 3 [13], where *H(s)* is the transfer function of the HVDC damping controller. From Figure 3 we can obtain the electric torque provided by the HVDC damping controller to the electromechanical oscillation loop of the generator to be:

$$\Delta T_{HVDC} = \frac{K_c(\lambda_0) K_0(\lambda_0) H(\lambda_0)}{1 - K_{IL}(\lambda_0) H(\lambda_0)} \Delta\omega \tag{24}$$

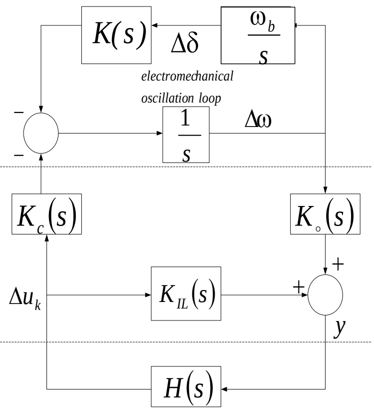

Figure 3. Closed-loop system installed with UPFC dumping controller

An ideal UPFC damping controller should contribute a pure positive damping torque to the electromechanical oscillation loop with $\Delta T_{HVDC} = D_{HVDC} \Delta\omega$ that is:

$$D_{HVDC} = \frac{K_c(\lambda_0) K_0(\lambda_0) H(\lambda_0)}{1 - K_{IL}(\lambda_0) H(\lambda_0)} \tag{25}$$

which results in:

$$D_{HVDC} = [K_c(\lambda_0) K_0(\lambda_0) + D_{IPFC} K_{IL}(\lambda_0)] H(\lambda_0) \\ = F(\lambda_0) H(\lambda_0) \tag{26}$$

$F(\lambda_0)$ which is named as the forward path of the BtB VSC HVDC damping controller, has a decisive influence on the effectiveness of the HVDC damping controller.

If we assume the set of the operating conditions of the power system is $\Omega(\mu), F(\lambda_0)$ can be denoted as the function of system operating condition μ and input control signal of the HVDC u_k. The criterion of the selection can be [14]:

$$\mu_{selected} = \min_{\mu} F(\lambda_0, \mu, u_k), \mu \in \Omega(\mu) \tag{27}$$

$$u_{selected} = \max_{u_k} F(\lambda_0, \mu_{selected}, u_k) \\ u_k \in \{M_r, M_i, PH_r, PH_i\} \tag{28}$$

$$uselected = \min_{u_k}\{\max_{\mu} F(\lambda_0, \mu, u_k) - \min_{\mu} F(\lambda_0, \mu, u_k)\} \\ u_k \in \{M_r, M_i, PH_r, PH_i\}, \\ \mu \in \Omega(\mu) \tag{29}$$

Equation (27) requires that the operating condition, where the HVDC damping control is least effective, is selected for the design of the controller.

- For the efficient operation of the HVDC damping function. The required damping should be provided at minimum control cost.

- A good design of damping controller requires that it provides a steady damping over all the range of power system operating conditions.

Furthermore, from Equation 26 we can see that the phase compensation method can be used to set the parameters of the HVDC damping controller.

IV. SIMULATION RESULTS

Power system information is given in appendix A. constant coefficients in (23) are calculated according information's who given in appendix B. For given information, characteristic equation is:

$$\Delta(s) = s^5 + 67.13s^4 + 684.7s^3 + 799.9s^2 + 9089s + 28180$$

with poles:

$-54.8593,\ 1.2442 \pm 3.8027j,\ -2.6505,\ -12.1114$

According above, there are two poles with positive real part and power system is unstable (for $\Delta P_e = 0.05$)

Figure 4 shows the damping of the oscillation mode over the $\Omega(\mu)$. It can be seen that, at the heavy load operating condition, the oscillation mode is of poorest damping. Therefore this operating condition is selected to design the damping controller.

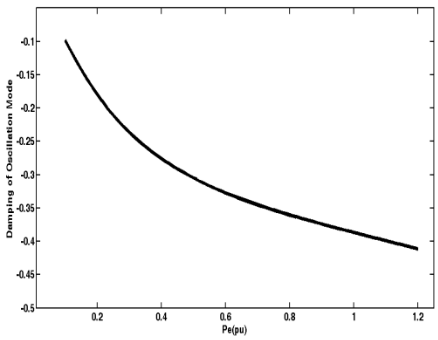

Figure 4. Damping of oscillation mode over the operating condition

The results of calculation of the forward path $F(\lambda)$ over $\Omega(\mu)$ as shown by Figure 5.

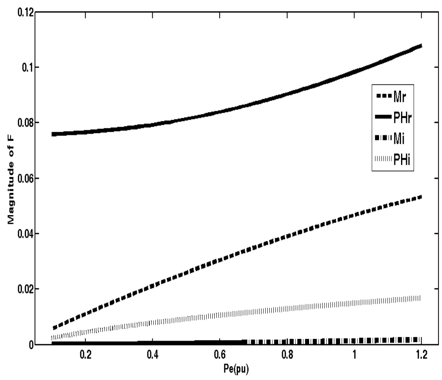

Figure 5. Magnitude of $F(\lambda)$ over $\Omega(\mu)$

➢ With $u_k = M_i$ we have $F(\lambda) \approx 0$ over $\Omega(\lambda)$. Therefore, the oscillation mode controllability is not controllable if the input control signal is chosen to be M_i. In the following M_i will not be included in the discussion.

➢ According to the criteria of Equation (26), it can be seen that the operating condition to be selected for the design of the HVDC damping controller is $P_e = 0.1$pu .

➢ Figure5, indicate $u_k = PH_r$ is most effective input control signal. So the criteria of Equation 28 lead to the selection of the input control signal for the UPFC damping controller as $u_k = PH_r$.

The results of applying the criteria of Equation 29 are:

with $u_k = PH_r$:

$$\frac{\max_\mu F(\lambda_0,\mu,u_k) - \min_\mu F(\lambda_0,\mu,u_k)}{\min_\mu F(\lambda_0,\mu,u_k)} = 0.44$$

with $u_k = M_r$:

$$\frac{\max_\mu F(\lambda_0,\mu,u_k) - \min_\mu F(\lambda_0,\mu,u_k)}{\min_\mu F(\lambda_0,\mu,u_k)} = 7.66$$

with $u_k = PH_i$:

$$\frac{\max_\mu F(\lambda_0,\mu,u_k) - \min_\mu F(\lambda_0,\mu,u_k)}{\min_\mu F(\lambda_0,\mu,u_k)} = 5.8$$

Therefore, with $u_k = PH_r$, the HVDC damping controller provides the smoothest damping to the oscillation mode. The final result of selection is:

$\mu_{selected} : P_e = 0.1$

$u_k = PH_r$

According to Figure 5 in $\mu_{selected}$, magnitude of F is very low. With attention to Equation 26, this reason decrease D_{HVDC} . So we select $\mu : Pe = 0.9$pu for damping controller designing. Using phase compensation method for damping controller results:

Table 1. Parameters of designed controllers

	M_r	PH_r	PH_i
T_1	0.31	0.19	6.2
T_2	0.36	0.59	0.018
K_{dc}	-60.91	-72.679	9.542

To assess the effectiveness of the damping controller two different conditions are considered according Table 2. Rotor speed deviation and electrical power for suddenly change in mechanical power ($\Delta P_m = 0.05$) is shown in Figure 6.

Table 2. Load condition

Load condition	$P_e(pu)$	$Q_e(pu)$
μ_1	0.9	0.015
μ_2	1.1	0.3

Designed controllers are applied to every input in Figure 2 individually. It is observed that if controller is applied to ΔPH_r, rotor speed oscillation is damped better than others input. This supplementary controller is caused the system stability and damping oscillations.

V. CONCLUSIONS

In this paper, a dynamic model for a AC-DC power system is considered and damping controller is designed for improve power system stability and oscillation damping. Damping function is defined and has been employed to evaluate the oscillation mode controllability to the four BtB VSC HVDC input. Results illustrated that the oscillation mode has best controllability via the fire angle of rectifier.

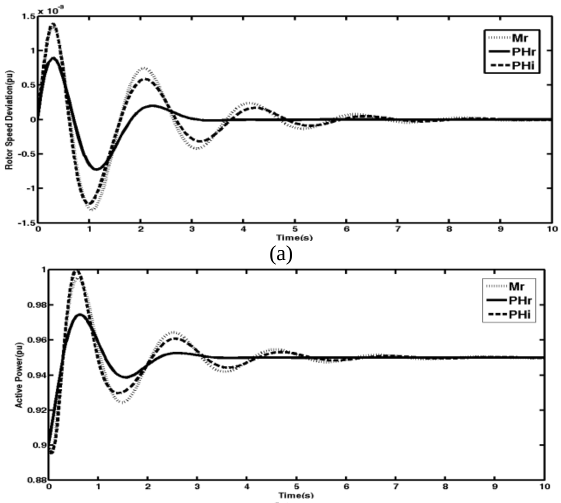

(a) (b)

Figure 6. μ_1 condition (a) Rotor speed deviation (b) Active power

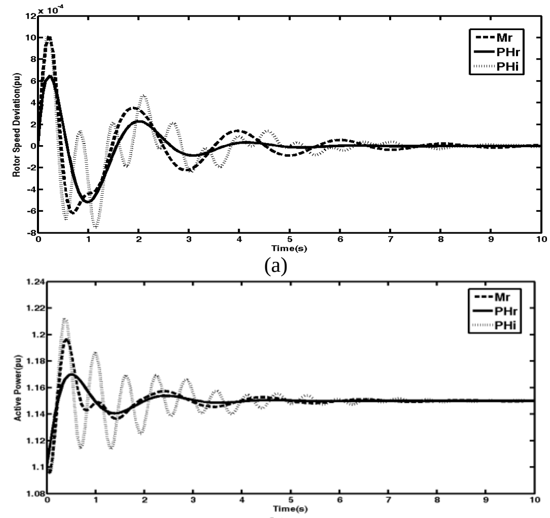

(a) (b)

Figure 7. μ_2 condition (a) Rotor speed deviation (b) Active power

APPENDICES

Appendix 1

The test system parameters are:

Machine and exciter:	$X_d = 1, X_q = 0.6, X'_d = 0.3, D = 0, M = 8,$ $T'_{do} = 5.044,\ freq = 60, v_{ref} = 1, K_A = 120,$ $T_A = 0.015$
Transmission line and transformer reactance:	$X_{tl} = 0.15, X_{lb} = 0.6,$ $X_{sp} = X_s = 0.15$
BtB VSC HVDC:	$V_{dc} = 3, C_{dc} = 1$

Appendix 2

Coefficients are:

$$Z = 1 + \frac{X_{lb}}{X_s},\ A = X_{tl} + X_{lb} + \frac{X_{tl}}{X_s},$$

$$[A] = A + ZX'_d,\ [B] = A + ZX_q$$

$$C_1 = \frac{V_b \cos(\delta)}{[B]},\ C_2 = -\frac{X_{lb} M_r V_{dc} \sin(PHr)}{2X_s[B]}$$

$$C_3 = \frac{X_{lb} V_{dc} \cos(PHr)}{2X_s[B]},\ C_4 = \frac{X_{lb} M_r \cos(PHr)}{2X_s[B]}$$

$$C_5 = \frac{Z}{A},\ C_6 = \frac{V_b \sin(\delta)}{[A]}$$

$$C_7 = -\frac{X_{lb} M_r V_{dc} \cos(PHr)}{2X_s[A]},\ C_8 = -\frac{X_{lb} V_{dc} \sin(PHr)}{2X_s[A]}$$

$$C_9 = -\frac{X_{lb} M_r V_{dc} \cos(PHr)}{2X_s[A]},\ C_b = E'_q + (X_q - X'_d)$$

$$C_a = (X_q - X'_d) I_{tlq},\ K_1 = C_b C_1 + C_a C_6$$

$$K_2 = I_{tlq}(1 + (X_q - X'_d) C_5),\ K_{pdc} = C_b C_4 + C_a C_9$$

$$K_{pMr} = C_b C_3 + C_a C_8,\ K_{pPHr} = C_b C_2 + C_a C_7$$

$$X_d - X'_d = J,\ K_3 = 1 + JC_5,\ K_4 = JC_6,\ K_{qPHr} = JC_7$$

$$K_{qMr} = JC_8,\ K_{qdc} = JC_9,\ L = \frac{1}{V_t}$$

$$K_5 = L(V_{td} X_q C_1 - V_{tq} X'_d C_6)$$

$$K_6 = LVtq(1 - X'_d C_5),\ K_{Vdc} = L(V_{td} X_q C_4 - V_{tq} X'_d C_9)$$

$$K_{VMr} = L(V_{td} X_q C_3 - V_{tq} X'_d C_8)$$

$$K_{VPHr} = L(V_{td} X_q C_2 - V_{tq} X'_d C_7),\ E = \frac{X'_d + X_{tl}}{X_s}$$

$$G = \frac{\sin(PHr)}{X_s},\ C_{10} = \frac{1}{X_s}(-(X'_d + X_{tl}) C_5 + 1)$$

$$C_{11} = -EC_6,\ C_{12} = -(EC_7 + \frac{M_r V_{dc} \cos(PHr)}{2X_s})$$

$$C_{13} = -(EC_8 + \frac{GV_{dc}}{2}),\ C_{14} = -(G\frac{M_r}{2} + EC_9)$$

$$W = \frac{X_q + X_{tl}}{X_s},\ C_{15} = -WC_1$$

$$C_{16} = -(WC_2 + \frac{M_r V_{dc} \sin(PHr)}{2X_s}),$$

$$C_{17} = -(WC_4 - \frac{M_r \cos(PHr)}{2X_s}),\ P_1 = -\frac{V_b \sin(\delta)}{X_{sp}}$$

$$C_{18} = -(WC_3 - \frac{V_{dc} \cos(PHr)}{2X_s}),\ P_2 = -\frac{M_i V_{dc} \cos(PHi)}{2X_{sp}}$$

$$P_3 = -\frac{M_i \sin(PHi)}{2X_{sp}},\ P_4 = -\frac{V_{dc} \sin(PHi)}{2X_{sp}}$$

$$P_5 = -\frac{V_b \cos(\delta)}{X_{sp}},\ P_6 = -\frac{M_i V_{dc} \sin(PHi)}{2X_{sp}}$$

$$P_7 = \frac{M_i \cos(PHi)}{2X_{sp}}, \; P8 = \frac{V_{dc} \cos(PHi)}{2X_{sp}}$$

$$P_9 = \frac{I_{lod} \cos(PHr) + I_{loq} \sin(PHr)}{2C_{dc}}$$

$$P10 = \frac{I_{bopd} \cos(PHi) + I_{lopq} \sin(PHi)}{2C_{dc}}$$

$$P_{11} = \frac{M_r \cos(PHr)}{2C_{dc}}, \; P_{12} = -\frac{M_r \sin(PHr) I_{lod}}{2C_{dc}}$$

$$P_{13} = \frac{M_r \sin(PHr)}{2C_{dc}}, \; P_{14} = \frac{M_r \cos(PHr) I_{loq}}{2C_{dc}}$$

$$P_{15} = \frac{M_i \cos(PHi)}{2C_{dc}}, \; P_{16} = -\frac{M_i \sin(PHi) I_{bopd}}{2C_{dc}}$$

$$P_{17} = \frac{M_i \sin(PHi)}{2C_{dc}}, \; P_{18} = \frac{M_i \cos(PHi) I_{bopq}}{2C_{dc}}$$

$$P_{124} = P_{12} + P_{14}, \; P_{186} = P_{18} + P_{16}$$

$$q_1 = P_{11}C_{11} + P_{13}C_{15} + P_{15}P_1 + P_{17}P_5$$

$$q_2 = P_{11}C_{10}, \; q_3 = P_{11}C_{14} + P_{13}C_{17} + P_{15}P_3 + P_{17}P_7$$

$$q_4 = P_9 + P_{11}C_{13} + P_{13}C_{18}, \; q_5 = P_{11}C_{12} + P_{13}C_{16} + P_{124}$$

$$q_6 = P_{10} + P_{15}P_4 + P_{17}P_8$$

$$q_7 = P_{15}P_2 + P_{17}P_6 + P_{186}$$

REFERENCES

[1] D.K. Chaturvedi, O.P. Malik and P.K. Kalra, “Performance of a Generalized Neuron Based PSS in a Multimachine Power System”, IEEE Transaction, 0885-8969/04, 2004.

[2] D.K. Chaturvedi, O.P. Malik and P.K. Kalra, “Performance of a Generalized Neuron Based PSS in a Multimachine Power System”, IEEE Transaction, 0885-8969/04, 2004.

[3] H.F. Wang and F.J. Swift, “A Unified Model for the Analysis of FACTS Devices in Damping Power System Oscillations Part I: Single-machine Infinite-Bus Power Systems”, IEEE Transaction, Power Delivery, Vol. 12, No. 2, pp. 941-946, Apr. 1997.

[4] N. Yang, Q. Liu, and J.D. McCalley, “TCSC Controller Design for Damping Interarea Oscillations”, IEEE Transaction, Power Systems, Vol. 13, No. 4, pp. 1304-1310, Nov. 1998.

[5] E. Uzunovic, C.A. Canizares and J. Reeve, “EMTP Studies of UPFC Power Oscillation Damping,” Proc. of NAPS’99, pp. 155–163, San Luis Obispo, California, Oct. 1999.

[6] X.M. Villablanca, J. del Valle, J. Rojas, J. Abarca and W. Rojas, “A Modified Back-to-Back HVDC System for 36-Pulse Operation”, IEEE Transaction, Vol. 15, No. 2, April 2000.

[7] K.R. Padylar, “HVDC Power Transmission Systems, Technology and System Interactions”, John Wiley & Sons, 1990.

[8] A. Hammad and C. Taylor, “HVDC Controllers for System Dynamic Performance”, IEEE Transaction on Power System, Vo1. 6, No. 2, pp. 743-752, May 1991.

[9] J.O. Gjerdc, R. Flolo and T. Gjengeddal, “Use of HVDC and FACTS Components for Enhancement of Power System Stability”, 8th Mediterranean Electro technical Conf., MELECON 96, Vol. 2, pp. 802-808, May 1996.

[10] G.M. Huang and V. Krishnaswamy, “HVDC Controls for Power System Stability”, IEEE Power Eng. Society Summer Meeting, Vol. 1, pp. 597-602, July 2002.

[11] M. Baker, K. Abbott and B. Gemmell, “Frequency and System Damping Assistance from HVDC and FACTS Controller”, Power Engineering Society Summer Meeting, IEEE, Vol. 2, pp. 770-773, July 2002.

[12] S. Corsi, et al., “Emergency Stability Controls through HVDC Links”, IEEE Power Eng. Society Summer Meeting, Vol. 2, pp. 774-779, July 2002.

[13] E.V. Larsen, J.J. Sanchez-GASCA and J.H. Chow, “Concept for Design of FACTS Controllers to Damp Power Swings”, IEEE Trans., PWRS-2, (10), pp. 948-956, 1995.

[14] H.F. Wang, “Damping Function of Unified Power Flow Controller” IEE Proc.-Gener. Transm. Distrib., Vol. 146, No. I, January 1999.

BIOGRAPHIES

Naser Mahdavi Tabatabaei was born in Tehran, Iran, 1967. He received the B.Sc. and the M.Sc. degrees from University of Tabriz (Tabriz, Iran) and the Ph.D. degree from Iran University of Science and Technology (Tehran, Iran), all in Power Electrical Engineering, in 1989, 1992, and 1997, respectively. Currently, he is a Professor of Power Electrical Engineering at International Ecoenergy Academy, International Science and Education Center and International Organization on TPE (IOTPE). He is also an academic member of Power Electrical Engineering at Seraj Higher Education Institute and teaches Power System Analysis, Power System Operation, and Reactive Power Control.
He is the secretaries of International Conference and Journal on TPE (ICTPE, IJTPE). His research interests are in the area of Power Quality, Energy Management Systems, ICT in Power Engineering and Virtual E-learning Educational Systems. He is a member of the Iranian Association of Electrical and Electronic Engineers (IAEEE).

Naser Taheri received the B.Sc. from University of Guilan (Rasht, Iran) in Electronics Engineering, 2007 and the M.Sc. degree from Azarbaijan University of Tarbiat Moallem (Tabriz, Iran) in Power Electrical Engineering, 2009. He is currently researching on Power System Control, Flexible AC Transmission Systems (FACTS) and Power Systems Dynamic Modelling.

Narges Sadat Boushehri received the B.Sc. from Sharif University of Technology (Tehran, Iran) in Control Engineering and Islamic Azad University, Central Tehran Branch in Electronic Engineering, 1991 and 1996 and the M.Sc. degree from International Ecocenergy Academy (Baku, Azerbaijan) in Electronic Engineering, 2009. She is currently researching on Power System Control and Artificial Intelligent Algorithms.